Physiological studies to optimize growth of the prototype biosolar cell factory Synechocystis sp. PCC6803

van Alphen, P.

Citation for published version (APA):
van Alphen, P. (2017). *Physiological studies to optimize growth of the prototype biosolar cell factory Synechocystis sp. PCC6803*.

2 Increasing the photoautotrophic growth rate of *Synechocystis* sp. PCC6803 by identifying the limitations of its cultivation

Pascal van Alphen, Hamed Abedini Najafabadi, Filipe Branco dos Santos, Klaas J. Hellingwerf

Abstract

Many conditions have to be optimized in order to be able to grow the cyanobacterium *Synechocystis* sp. PCC6803 (*Synechocystis*) for an extended period of time under physiologically well-defined and constant conditions. It is still poorly understood what limits growth in batch and continuous cultivation in BG-11, the standard medium used to grow *Synechocystis*. A complicating factor is the tendency of BG-11 to form a copious precipitate in the medium reservoir, hampering continuous cultivation. Through a series of batch experiments in flasks and continuous mode experiments in photobioreactors, we show that the limiting nutrient in batch cultivation is sulfate, the depletion of which leads to ROS formation and rapid bleaching of pigments after entry into stationary phase. Optimizing these growth conditions resulted in a growth rate of $0.16 \, h^{-1}$ (4.3 h doubling time) in continuous, steady-state cultivation, which is significantly higher than the textbook value of $0.09 \, h^{-1}$ (8 h doubling time). We present an improved medium, BG-11 for prolonged cultivation (BG-11-PC) that solves precipitation issues. The data we present allow for controlled, extended cultivation of *Synechocystis,* under well-defined physiological conditions, and have implications for mass-culturing of cyanobacteria.

2.1   Introduction

Cyanobacteria, as primary producers, play an important role in solar-energy conversion and the carbon cycle on Earth (28). Several representatives of this class of organisms have been intensely studied, of which the strain *Synechocystis* sp. PCC6803 (*Synechocystis*) has become a model organism for the elucidation of the molecular basis of oxygenic photosynthesis, due to its amenability to genetic modification, early availability of its genome sequence and ability to grow heterotrophically (11, 132, 133). During the past decade, increased interest in the application of microalgae for the transition of society to a sustainable bio-based economy is reflected in an increase in efforts to mass-culture microalgae, including cyanobacteria. The latter is done both for biomass production and for direct conversion of CO_2 into (commodity) products (21, 57). This recent bloom of cyanobacterial research has also led to an increase in our understanding of how to culture cyanobacteria like *Synechocystis*. This requires optimization of conditions such as temperature, light intensity and medium composition, which, surprisingly, are unknown still for a large number of (cyano)bacteria, many of which have remained non-cultivable in the lab (134). Of these conditions, the medium composition is of particular importance. Since the pioneering work carried out between 1940 and 1980, the period in which the composition of the most commonly used medium for growth of cyanobacteria, BG-11, was formulated, little further optimization has been done. As a result, the medium according to Rippka *et al*. (1979) has become the medium of choice, with only few exceptions (135-138).

A known, but mostly ignored, aspect of the BG-11 medium is its tendency to develop a yellowish precipitate (135). Formation of such a precipitate is not obvious in batch cultures in Erlenmeyer flasks (hereafter called flasks), but precipitate formation is particularly troublesome in experiments using continuous culturing systems, in which fresh medium has to be stored for days, or even weeks, in a reservoir bottle. As noted by Keren and coworkers (2007), such a precipitate defeats the purpose of a chemically defined medium and hampers any research involving defined concentrations of trace metals such as iron, which is prone to precipitate on the cell surface (138). Additionally, the medium composition of course defines to which rate and extend growth can be supported, and influences the composition of the resulting biomass and the metabolic state of the cells (139-142).

A further complicating factor, which has already been pointed out by Kratz & Myers (1955) is the lack of buffering capacity of (what eventually became) BG-11, which makes it necessary to add a buffer if a specific pH is to be maintained. Unfortunately, in many recent publications the pH during culturing is poorly defined, or assumed to stay constant with minimal buffering of the medium, in combination with aerating the growing culture with ambient air for CO_2 supply. Considering the buffering capacity at pH 8.0 of 10 mM 4-(2-Hydroxyethyl)-1-piperazineethanesulfonic acid (HEPES), a commonly used buffer, and assuming that approximately 13 % of the cellular dry weight is nitrogen (143), it follows

that assimilation of (sodium) nitrate, which increases alkalinity in the medium, will completely exhaust the buffering capacity of the HEPES as early as when a dry biomass content of 0.3 g L^{-1} has been reached. This amount of biomass contains only about 15 % of the available nitrogen in BG-11. Similarly, light intensity (and quality) is a critical culturing parameter for a photoautotroph such as *Synechocystis,* but is frequently meekly defined as 'low', 'moderate' or 'high'. Alternatively, an incident light intensity is given without further specifying optical density, flask geometry, or culture volume. Furthermore, certain parameters that play almost no role in culturing in shake flasks, do have a significant influence during cultivation in photobioreactors, such as shear stress (due to e.g. stirring and sparging (144)) or high pO_2 and low pCO_2 in the liquid phase due to poor mass transfer.

In this study, we define which mineral nutrient limits growth in BG-11-PC in batch and continuous culture and describe optimized conditions in which high growth rates can be achieved and sustained. We propose an improved composition of the BG-11 medium, named 'BG-11 suited for prolonged cultivation' (BG-11-PC) with suggestions on how to adapt the medium composition to avoid specific limitations. This new medium eliminates precipitation issues by increased chelation of poorly soluble metal ions and allows for buffering through controlling alkalinity and pCO_2. We describe in detail the culturing conditions that have been used to arrive at these conclusions.

2.2   Materials and Methods

2.2.1   Strain and growth conditions

The glucose tolerant (GT), non-motile variant of *Synechocystis* variant derived from the Williams GT *Synechocystis* strain was obtained from D. Bhaya (Carnegie Institution for Science, Stanford, USA). To avoid accumulation of mutations in this strain, cells were re-streaked once per month on solidified agar plates (described below) from stocks kept in 5 % (v/v) DMSO at -80 °C and placed in an incubator (Versatile Environmental Test chamber MLR-350H, Panasonic, Japan) equipped with fluorescent white lamps, resulting in approximately 50 µmol photons m^{-2} s^{-1}, as measured with a LI-250 quantum sensor (LI-COR, USA). The incubator was kept humidified and at elevated pCO_2 (2 % v/v) at 30 °C.

Flask experiments were conducted in a shaking incubator (Innova 44, New Brunswick Scientific) equipped (in the top cover) with a custom-designed LED panel containing 632 nm orange-red and 451 nm blue LEDs (both with 15 nm FWHH). Cultures of 25 mL were grown in 100 mL flasks (FB33131, Thermo Fisher Scientific, USA) with paper stoppers (Stopper Cellulose, VWR, USA), at 30 °C and 120 rpm under ~30 µmol photons m^{-2} s^{-1} combined incident light intensity of orange-red and blue light (10 : 1 ratio), unless noted otherwise. Samples of 25 to 800 µL were taken, depending on the expected optical density at 730 nm (OD$_{730}$) of the culture and the required dilution factor to obtain a measured OD$_{730}$ in the linear range of the benchtop photospectrometer used (i.e. from 0.10 to 0.70, Lightwave II, Biochrom, USA). Pre-cultures were grown for each condition tested.

2.2.2   Cell counting

Cell counts and cell size were measured using a CASY counter (CASY Model TTC, Roche, Switzerland), following the manufacturer's instructions. Briefly, samples diluted for OD_{730} measurements as described above were further diluted in 10 mL CASY ton in a CASY cup. Dilutions were made such that background counts contributed no more than 1 % of the counts with a maximum of 20,000 counts per 200 µL. The cumulative counts of three such measurements were used to calculate the cell counts mL^{-1} of a sample. The average size of all particles measured between 1.2 and 5 µm is reported as mean cell size of a particular sample. When applicable, both biological and technical replicates were averaged and the mean and standard deviation of a particular condition is presented.

2.2.3   Measurement of the cellular level of reactive oxygen species

Cultures were tested for the presence of reactive oxygen species (ROS) by addition of the ROS probe 2',7'-dichlorodihydrofluorescein diacetate (H_2DCFDA, Thermo Fisher Scientific, USA). 50 µL of a freshly prepared solution of H_2DCFDA (100 µM in BG-11-PC, 1 % (v/v) DMSO) was added to 450 µL sample, for a final H_2DCFDA concentration of 10 µM. The mixture was incubated for 45 min at 30 °C in the same incubator as used for cultivation. The fluorescence signal of the ROS probe was subsequently quantified using a flow cytometer (Accuri C6, BD, USA) on the FL1 channel (488 nm excitation, 533/30 nm emission filter).

2.2.4   Dry cell weight

Dry weight was determined gravimetrically by employing membrane filtration. Briefly, cellulose membranes with a pore size of 0.2 µm (Supor-200, Pall, USA) were washed using purified water (Milli-Q Reference, Merck Millipore, USA) and dried in an oven at 90 °C before being weighed with an analytical balance (AB204, Mettler Toledo, Switzerland). Next, a defined culture volume was filtered through the prepared membrane, which was subsequently washed using purified water, dried and weighed again. The resulting DW was normalized by OD_{730} and volume to obtain gDW OD_{730}^{-1} L^{-1}. For flask experiments, biological replicates were measured once and averaged for the reported mean and standard deviation per condition. For chemostats, it was measured in technical triplicate and reported as the mean with standard deviation.

2.2.5   Growth medium

BG-11 (145) was modified to be chemically defined and suited to accommodate prolonged cultivation in a PBR with CO_2/(bi)carbonate-based buffering (Supporting Information **Table S2.1**). Hereafter this modified medium is referred to as BG-11-PC. To better define the iron content and remove citrate altogether from the medium, ferric ammonium citrate and citric acid were replaced by $FeCl_3 \cdot 6H_2O$ (15 µM) and an increased concentration of ethylenediaminetetraacetic acid (EDTA) to 50 µM in the final iteration of the medium. The final pH of this medium is approximately 6, necessitating a buffer to obtain conditions compatible with the requirements of *Synechocystis*. For experiments in a PBR, 10 mM fresh $NaHCO_3$ was added to the medium to provide a carbon-rich environment in which

the pH is controlled by manipulating the pCO_2 in the gas mixture used to sparge the culture. In flask experiments, 50 mM 1,4-Piperazinedipropanesulfonic acid (PIPPS, Merck Millipore, USA)-KOH, buffered at pH 8.0, was used instead of 10 mM $NaHCO_3$, unless noted otherwise. PIPPS has a pK_a close to 8 at 30 °C (7.96 and 7.86 at 25 and 35 °C, respectively (146)) and was described as a non-metal-complexing buffer that fulfills Good's criteria (147) and is similar in structure to the commonly used HEPES.

2.2.6   Photobioreactors

Continuous cultivation experiments were conducted in PBRs of the types FMT 150.2/1000 and FMT 150.2/400 (Photon Systems Instruments, Czech Republic, hereafter PSI), with 960 and 395 mL working volume, respectively, controlled using the ADVANCED version of the control software provided by PSI. The PBRs were configured as described in detail before (148), with slight modifications. Specifically, the U-shaped standard sparger (4 orifices, diameter 0.7 mm) of the PBRs was replaced by a custom-made L-shaped variant (8 orifices, diameter 0.7 mm) that requires only 1 of the threaded Luer Lock connectors in the lid of the PBR. The end of the sparger tube is closed to the extent that most, but not all, of the gas is forced through the defined orifices. In order to avoid the strong variation in bubble size and distribution that can be observed when using the default sparger, the new one was designed to have all orifices directly below the stirring bar (Supporting Information **Fig. S2.3**). The rate of the magnetic stirrer (PSI) was set at 50 % in all experiments. The 4 Luer Lock connectors in the lid of the PBR are respectively used for: sparging and medium feed, effluent and gas exhaust, sampling, and inoculation. A stream of CO_2 and N_2, mixed by a software-controlled gas mixer (GMS 150, PSI), was used to sparge the PBRs. In experiments in which pH was maintained at a certain value, the CO_2 valve of the gas mixer was controlled by a dedicated script, otherwise a constant mix of 1 % (v/v) CO_2 in N_2 was used, yielding a pH between 7.9 and 8.3, depending on the growth rate and biomass density. In turbidostat experiments, an $OD_{730} = 0.4$ (OD_{730} of 1 approximately equals 0.18 g dry weight(DW) L^{-1} under the presented conditions) as measured on a benchtop photospectrometer was maintained, ±2.5 % for the upper and lower bounds, unless noted otherwise. Temperature was maintained at 30 ±0.1 °C unless noted otherwise. In chemostat experiments, the flow rate set by the medium pump (PP500, PSI) was regularly checked by measuring the volume pumped using a pipette that was integrated in the setup, at the same height as the medium reservoir. Steady-state was assumed when biomass density remained constant within a few percent (< 2 %) during 5 volume changes. Light intensity was measured outside the PBR, in the middle of the light panel. Actual intensities used varied and are specified for the respective experiments. For a general description of these PBRs the reader is referred to Nedbal *et al*. (2008).

A second setup consisted of a flat-panel glass vessel (2.5 cm light path length) of approximately 220 mL working volume, which was placed in a transparent water bath kept at 30 ±0.5 °C (149). Directly in front of the water bath, an LED panel integrated with a heat sink and diffuser ('LED box'), of comparable size as the culture vessel, was used as

actinic light source. This custom-made LED box contains LEDs of various wavelengths (600, 635 and 660 nm, FWHH 15 nm), each controllable independently. Light intensity was measured on the outside of the vessel, opposite to the LED box in the middle of the panel. Similar to the FMT 150.2 PBR, the vessel was configured to have combined input for sparging and medium feed, a sampling port, and a combined outflow of effluent and gas exhaust. This reactor was sparged with a flow (~20 mL/min) of 3 % (v/v) CO_2 in N_2 and agitated by a magnetic stirrer on the bottom of the vessel. A peristaltic pump (Minipuls 2, Gilson, USA) was used to control the dilution rate in chemostat mode.

2.2.7 Elemental analysis

The precipitate that formed in ~60 L of modified BG-11 medium as described in van Alphen & Hellingwerf, 2015 (148), when supplemented with 10 mM $NaHCO_3$, was collected on a paper filter, washed with purified water (Milli-Q Reference, Merck Millipore, USA) water and dried in an oven at 60 °C. The resulting solid was dissolved in 4 M HCl, yielding a greenish solution, which was subsequently analyzed using inductively coupled plasma optical emission spectroscopy (ICP-OES, Optima 8000, PerkinElmer, USA). 200 mL of culture ($OD_{730} \approx 0.9$) was sampled from a chemostat ($D = 0.08$ h^{-1}) at steady-state. The sample was split in two and centrifuged (7,000 x g, 20 min). One half was washed with 10 mM EDTA, dissolved in 65 % (w/v) HNO_3 to a total of 6 mL and filtered (0.2 μm pore size filters) for ICP-OES analysis; the other half was washed with purified water and freeze-dried for CHN analysis (vario EL cube, Elementar, Germany). The approximated pellet volume of 10 mM EDTA, made up to 6 mL with HNO_3, was used as a control. For ICP-OES, two biological samples were collected and measured with five technical replicates each, for which the mean and standard deviation is reported. For CHN analysis, four technical replicates were measured, again reporting the mean along with standard deviation.

2.3 Results

In order to determine optimal growth conditions in continuous cultivation systems, several experiments were conducted, ranging from batch growth in flasks to extensively controlled continuous growth in a PBR. First, the technical challenges to reach controlled physiological conditions were tackled, after which selected properties of *Synechocystis* cells, grown under these conditions, were analyzed.

2.3.1 Insufficient chelation of ferric iron and calcium ions causes precipitation in BG-11 medium

In a previous study (148) we already used a modified version of BG-11 that was prepared along the lines of YBG-11, as described by Keren and coworkers (138), i.e. by replacing ammonium ferric citrate and citric acid with a well-defined iron source, ferric chloride, and increasing the concentration of EDTA from 2.8 to 15 μM. Despite this increase in EDTA concentration, addition of 10 mM $NaHCO_3$ to this medium still leads to formation of a powdery white-yellowish precipitate within a day at room temperature, interfering with continuous cultivation.
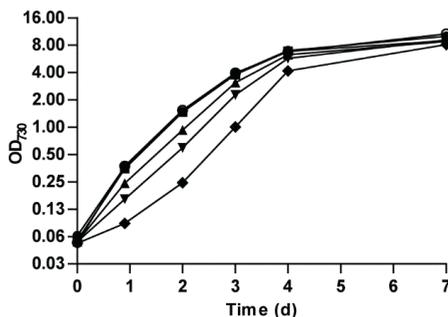
Fig. 2.1. Growth of Synechocystis in modified BG-11 medium with varying concentrations of EDTA added, as compared to growth in standard BG-11 (Sigma). Cultures were illuminated by approximately 70 µmol photons $m^{-2} s^{-1}$ orange-red and blue light (10 : 1 ratio), buffered by 200 mM 2-[[1,3-dihydroxy-2-(hydroxymethyl)propan-2-yl]amino]ethanesulfonic acid (TES) and regularly supplemented with 10 mM $NaHCO_3$ up to day 4. Note the Log_2 scale of the Y-axis. Closed circles: BG-11-PC with 15 µM EDTA total, squares: 50 µM, upward triangles: 100 µM, downward triangles: 150 µM, diamonds: 200 µM, open circles: Commercial Sigma BG-11. Note that open and closed circles and squares overlap over the entire growth curve. Mean and standard deviation are shown (n = 2). Error bars were smaller than the data symbols at all the time points.

The precipitate was analyzed with ICP-OES and found to contain mostly iron, calcium and phosphorus (data not shown). No gas formation was apparent upon its dissolution in HCl, which indicated that calcium precipitated with phosphate rather than with carbonate. Further increasing the concentration of EDTA prevented this precipitate from forming (data not shown). The effect of increased EDTA was tested in conditions that allow for rapid growth in batch culture (**Fig. 2.1**). Despite a clear lag phase of the culture growing with 200 µM EDTA, the growth rate increases to values similar to those seen with much lower concentrations of EDTA.

It should be noted that regular addition of $NaHCO_3$ was required to avoid a carbon-limited, high-light phenotype at the chosen light intensity of 70 µmol photons $m^{-2} s^{-1}$ of orange-red and blue light (10 : 1 ratio). Consequently, high buffering capacity was required to control the pH. The lowest tested concentration of EDTA (50 µM) at which neither a precipitate formed in the presence of 10 mM NaHCO3, nor a difference in growth characteristics could be observed relative to standard BG-11 medium, was selected as the concentration for subsequent experiments. It is relevant to note that while 50 µM EDTA has no measurable effect on the growth of *Synechocystis* in liquid medium, it is not suited for cultivation on agar plates, as this leads to poor or no growth (data not shown).

2.3.2 Sparging in photobioreactors causes shear stress and a distinct phenotype in *Synechocystis*

In previous work, we found that each PBR required a different sparge rate for reproducible growth (148), consistent with the observations of shear stress caused by sparging made by Barbosa and Wijffels (2004) in microalgae. To obtain reproducible sparging in the PBRs, a new sparger was designed (see Supporting Information **Fig. S2.3**).
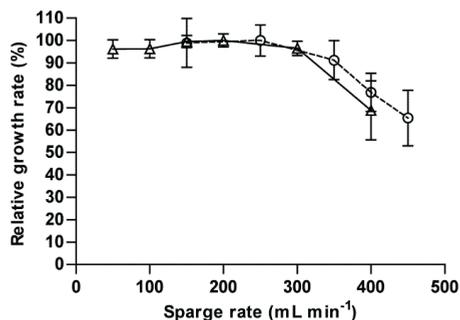
Fig. 2.2. Growth rate of *Synechocystis* in a photobioreactor in turbidostat mode is affected by sparging. Growth rate was normalized in both series to its respective maximum. Circles: average growth rate at 100 % equals 0.07 ±0.005 h^{-1} at 75 µmol photons m^{-2} s^{-1} orange-red light; triangles: 0.05 ±0.001 h^{-1}, 50 µmol photons m^{-2} s^{-1} orange-red light. Means with SD (error bars) of many (> 20) dilution cycles at a given sparge rate are shown.

The effect of sparging on growth rate was then investigated by examining cultures growing under different light intensity at the same density (i.e. yielding different growth rate). Sparging appears to affect growth rate similarly, irrespective of growth rate, showing that *Synechocystis* is sensitive to sparging (**Fig. 2.2**).

Interestingly, in turbidostat mode, at sufficiently high sparging rates, the OD continuous to drop even after the pump has stopped and growth, as measured via OD_{720} by the PBR (PBR_{720}), only slowly recovers (Supporting Information **Fig. S2.1**). Due to the small difference in OD and the relatively large error in dry weight measurements it is difficult to assess the corresponding differences in dry weight of the cells. We therefore could not determine whether this drop in OD is caused by an actual decrease of biomass content or by morphological changes of the cells that have an effect on light-scattering.

2.3.3 Cell size is affected by growth rate and by medium pH

Measurement of the optical density of a culture at a wavelength (well) beyond the maximal absorption wavelength of chlorophyll is a widely-accepted method of measuring volumetric biomass content of batch cultures of cyanobacteria during all phases of growth. However, because optical density is caused by light-scattering rather than by absorption, the size of the particles (i.e. the cells) that are measured, directly affects the outcome of the measurements. Therefore, we compared population growth recorded as OD_{730} and as the number of cells mL^{-1} (**Fig. 2.3**, panels **A** and **B**). From the OD_{730} it appears that cultures at higher pH grow faster, but when examining cell counts a different picture emerges. At pH 9, the increase in cell counts stagnates after about 7 days, even though the OD_{730} still increases; the latter gives the impression of continued growth, but in fact it is only cell size that increases and the cells no longer divide (**Fig. 2.3**, panels **C** and **D**). The cell size data shows greater variance in non-buffered than in buffered medium. This is reflected in the cell size distribution of any given sample of a particular condition.
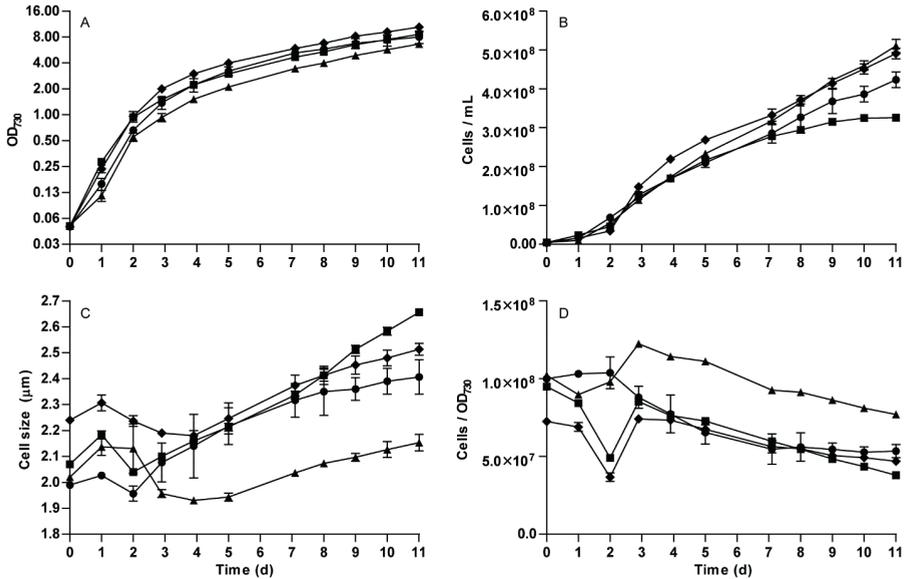
Fig. 2.3. Cell size affects optical density and is influenced by medium pH. Synechocystis was grown in modified BG-11, either non-buffered or buffered using 50 mM PIPPS (pH 8.0) or CAPSO (pH 9.0 and 10.0). (A) Growth curves based on optical density at 730 nm. Note the Log_2 scale of the Y-axis. (B) Cell count per mL (C) Cell size (µm) (D) Cell count per OD_{730}. Circles: non-buffered BG-11-PC, triangles: BG-11-PC buffered at pH 8.0, squares: pH 9.0, diamonds: pH 10.0. Mean and standard deviation are shown (n = 3). Where no error bar is visible, it is smaller than the data symbol.

Whereas growing cells at pH 8.0 results in a single clear peak with the shape of a skewed Gaussian curve over the whole growth curve, other conditions, notably non-buffered ones, lead to the observation of multiple peaks, indicative of multiple sub-populations of cells (data not shown). Despite these differences, gDW OD_{730}^{-1} L^{-1} is approximately equal for all cultures at the end of the experiment on day 10 (0.18 ±0.01), indicating that the OD_{730} can provide a good indication of dry weight, but not of cell count.
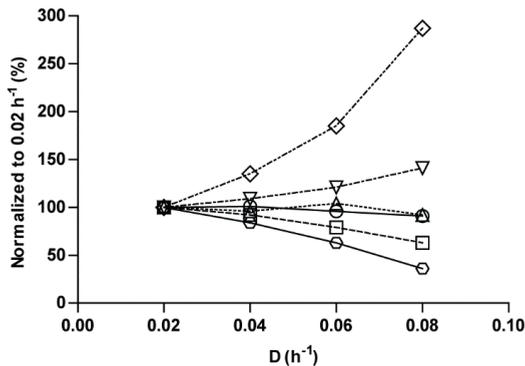

Fig. 2.4. Cell size increases with growth rate. Values are given relative to the value at the dilution rate of 0.02 h^{-1}. Circles: OD_{730} (0.52 at 0.02 h^{-1}), squares: PBR_{720} (0.31), upward triangles: gDW OD_{730}^{-1} L^{-1} (0.18), downward triangles: cell diameter (1.90 µm), diamonds: cell volume (3.91 fL), hexagons: cell count mL^{-1} (5.5 * 10^7).

Interestingly, there is a clear shift in cell size after growth has slowed down to a certain extent, though far before cells enter stationary phase.

In order to determine the relation between growth rate and cell size for *Synechocystis*, PBRs were run as a light-limited chemostat at various dilution rates (**Fig. 2.4**). Light intensity was scaled with dilution rate so as to maintain an equal perceived light flux for the cells at all dilution rates, i.e. 25, 50, 75 and 100 μmol photons m^{-2} s^{-1} at 0.02, 0.04, 0.06 and 0.08 h^{-1}, respectively (150). As in flask experiments, gDW OD_{730} $^{-1}$ L^{-1} is approximately constant, despite big differences in cell size (see upward triangles). This is in stark contrast with the PBR_{720}, which showed strong changes with dilution rate for unknown technical reasons, though this again emphasizes that optical density can be misleading as a measure of biomass density if not verified with dry weight. Parallel to increasing cell size with increasing growth rate, chlorophyll content (i.e. antenna/photosystem content) decreases as growth rate increases (data not shown).

2.3.4 Sulfate limitation leads to ROS formation followed by bleaching and death of *Synechocystis* in BG-11 medium

In batch cultures of *Synechocystis* in BG-11, if the cells are allowed to enter stationary phase, this phase is followed by a death phase in which all cellular pigments rapidly bleach and OD_{730} decreases. In order to determine what limits the maximal amount of biomass that can be formed in such batch cultures, all individual nutrients from BG-11-PC were tested by reducing them two-fold, while keeping all others at the original level (Supporting Information **Table S2.2**). Additionally, various metals were tested that may be required but are not explicitly added to BG-11 and if limiting, addition of trace amounts, well below toxicity limits, is expected to sort an obvious effect. One such metal is nickel, which has been shown to be required for growth (151). The results of these tests show that maximum OD_{730} correlates only with magnesium sulfate content; addition of non-standard metals did not make a difference. Furthermore, two-fold reduction of the concentration of sodium nitrate resulted in a culture with a different phenotype than that of all other cultures. Whereas typically a maximum OD_{730} is reached, after which it drops again in parallel with pigment bleaching, instead, in a medium with a lowered nitrogen content, the OD_{730} continues to increase as the phycobilisomes are degraded and a small chlorophyll peak remains (Supporting Information **Table S2.2**, and data not shown).

Because limitation by magnesium sulfate may be due to either magnesium or sulfur, a follow-up experiment was done to separately investigate the requirement for these elements (**Fig. 2.5a**). The result of this experiment clearly shows that sulfate is the limiting nutrient in BG-11-PC, as well as in BG-11. Given that cultures that reach stationary phase in this way rapidly bleach of both phycobilisomes and chlorophyll and that sulfur is a required element for various electron-transfer components, such as iron-sulfur clusters, and the ROS-scavenging machinery (152), we anticipated that ROS formation could play a role in this phenotype.
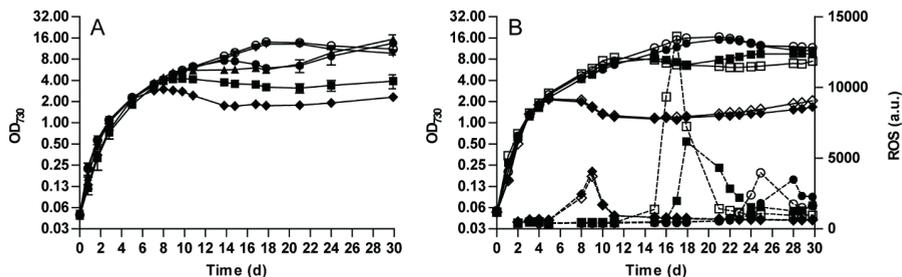
Fig. 2.5. The growth-limiting nutrient of *Synechocystis* in BG-11-PC in batch culture. Note the Log_2 scale of the y-axes. (A) Magnesium chloride and potassium sulfate replaced magnesium sulfate in BG-11-PC in various concentrations. Upward triangles: BG-11-PC with 0.125x magnesium, open circles: 0.22x magnesium, downward triangles: 0.5x magnesium, diamonds: 0.125x sulfate, squares: 0.22x sulfate, closed circles: 0.5x sulfate. On day 18, sulfate was added to all cultures with reduced-sulfate content and magnesium was added to 0.125-fold magnesium content. Means of duplicates (n = 2) with error bars (SD) are shown. Where no error bar is visible, it is smaller than the data symbol. (B) Sulfur limitation leads to ROS formation followed by bleaching and death of *Synechocystis*. Diamonds: BG-11-PC with 0.1x sulfate, squares: 0.5x sulfate, circles: 1x sulfate. Solid lines show the OD_{730} (left axis), dashed lines ROS (right axis). On day 16, sulfate was supplemented to 0.5x sulfate (squares). Duplicates of cultures are shown by open or closed symbols of the same type.

This was confirmed in experiments in which the ROS probe H_2DCFDA (153) was used: These experiments show a clear correlation between the appearance of ROS, the onset of stationary phase and the subsequent bleaching (**Fig. 2.5B**). In the cultures in which the sulfate concentration was reduced two-fold, additional sulfate was supplemented on day 16. This allowed for partial recovery of the culture with low ROS (closed squares) but had no effect on the culture in which the cells had already produced a high level of ROS (open squares, **Fig. 2.5B**). It is interesting to note that the recovering culture only slowly decreased ROS levels, reaching control values only in about two weeks.

The unexpected result of sulfate limited batch cultivation prompted the analysis of the elemental biomass composition (C:H:N:P:S) of cells of which we presume that they were as lean as possible regarding their cellular content of P, N and S; i.e. light-limited cells in steady-state chemostat at high dilution rate close to the textbook μ_{max} of 0.09 h^{-1} (0.08 h^{-1}). The mass ratios were found to be 45.12 ±0.18% : 8.58 ±0.50% : 10.80 ±0.04% : 1.94 ±0.02% : 0.44 ±0.01%. Additionally, the biomass was analyzed for nearly all elements added to the medium, as well as for various heavy metals and other rare elements (Supporting Information **Dataset 1**). The biomass composition that was found suggests that phosphorus should be limiting before sulfur. This is in line with the observation that in a non-light-limited chemostat, the residual phosphate concentration drops below the detection limit (data not shown).

2.3.5 Chemostat culturing allows for a higher maximum growth rate of *Synechocystis* than turbidostat mode

In an effort to find the maximum growth rate (μ_{max}, i.e. the growth rate in the absence of all nutrient limitation) of *Synechocystis*, a wash-out experiment was performed (154). A light-limited chemostat at a high dilution rate (0.08 h^{-1}, $OD_{730} \approx 0.5$, 120 µmol photons m^{-2}

s^{-1}), close to the observed μ_{max} in a steady-state turbidostat (i.e. ~0.09 h^{-1}) was switched to a dilution rate (0.2 h^{-1}) that exceeds the μ_{max} reported for *Synechocystis* (150, 155). This results in the washing-out of the cells and progressively increases perceived light intensity of the remaining cells until light is no longer limiting and μ_{max} is reached. At this point, the wash-out becomes exponential (i.e. gives a straight line on a log scale). This allows one to calculate μ_{max} from the resulting slope and the known dilution rate. This experiment was repeated using monochromatic light of various wavelengths in the orange-red range and yielded a surprisingly high growth rate of up to 0.15 h^{-1} that was constant over at least 5 hours (data not shown).
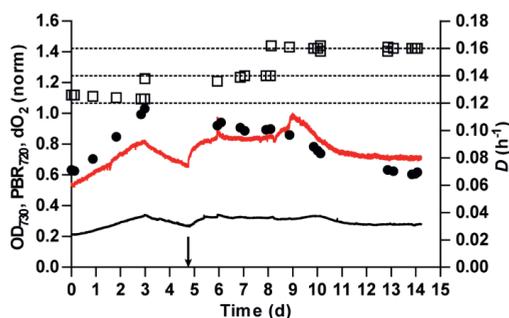

Fig. 2.6. Steady-state growth of *Synechocystis* in a chemostat at dilution rates up to 0.16 h^{-1} at 350 µmol photons m^{-2} s^{-1} orange-red light. The arrow marks the point in time when the temperature was increased from 30 to 32 °C. Filled circles: OD$_{730}$ (left axis), open squares: calculated D (right axis) at the time of sampling by measuring the rate of medium supply (set values are shown as dotted lines), OD$_{720}$ as measured by the PBR (PBR$_{720}$, black line, left axis) and dissolved O$_2$ normalized to the maximum measured (red line, left axis).

The possibility that the nature of a turbidostat regime, i.e. periodic strong dilution, is the underlying reason of a lower apparent μ_{max} was tested by choosing the turbidostat thresholds such that there are more periods of lesser dilution, thereby approximating chemostat conditions. Interestingly, this indeed had an effect and a culture growing in steady state in turbidostat mode increased its growth rate in response to this narrowing of the turbidostat range (Supporting Information **Fig. S2.2**). However, the question remained whether the high growth rates found in the wash-out experiment can be sustained, which was tested using regular chemostat cultivation (**Fig. 2.6**). Dilution rates up to 0.12 h^{-1} can be maintained at 30 °C; steady state at higher dilution rates requires an increase to 32 °C (**Fig. 2.6**, arrow). Even a dilution rate as high as 0.16 h^{-1} results in a stable steady state, confirming that such growth rates can indeed be sustained in chemostat mode.

2.4   Discussion

Here, we present a growth medium (BG-11-PC) for *Synechocystis* that allows for prolonged cultivation under chemically defined, continuous-growth conditions in PBRs. This was realized by replacing citrate and ammonium ferric citrate by ferric chloride and by increasing the concentration of EDTA to 50 µM. Omission of citrate has the additional

benefit of lowering the biologically available organic carbon content, thereby reducing the risk of mixotrophic growth and contamination with chemotrophic organisms. The increased concentration of EDTA is similar to, though lower than, the concentration of EDTA in a similar minimal mineral medium, A$^+$ (156). There turned out to be a notable downside to increasing the concentration of EDTA to concentrations much higher than 50 µM, i.e. the appearance of a long lag phase (**Fig. 2.1**). Pre-culturing under the same conditions would be expected to eliminate this apparent lag phase, observed at higher concentrations of EDTA; however, it did not. There is considerable evidence that siderophores are not produced by *Synechocystis* and that this organism mainly takes up free Fe^{3+} (157). Considering EDTA chelates other di- and trivalent cations as well, it may be that excreted chelators for these cations exist that have to be resynthesized upon dilution. It should be noted that initially 65 µM EDTA was selected, after occasionally a precipitate was detected at 50 µM, but this could be correlated to the age of the NaHCO$_3$ solution used. Because of the volatile nature of CO$_2$, it appears critical that fresh bicarbonate solutions are used to assure a pH near 8 (a fresh solution of 10 mM NaHCO$_3$ has a pH of 8.3), as the solubility of iron(III), and the ability of EDTA to chelate it, both decrease with increasing pH.

When operating a PBR, there often is a conflict between the need for vigorous sparging for a high mass-transfer rate of CO$_2$ and O$_2$ on the one hand, and low shear stress to cells on the other. For various algae, it was shown that the gas entrance velocity is the dependent variable, rather than bubble size or column height, that determines the detrimental effect of the shear stress (144). For *Synechocystis*, we show that high sparging rates similarly impact its growth rate (**Fig. 2.2**). In our turbidostat experiments, *Synechocystis* has consistently shown a μ_{max} of ~0.09 h^{-1}, with the notable exception described above (Supporting Information **Fig. S2.2**). In the same photobioreactor in chemostat mode, however, the organism is clearly capable of growing much faster (**Fig. 2.6**). This raises the question of what limits the growth rate of *Synechocystis* in any specific condition, and why this limitation cannot be overcome by cells growing in turbidostat mode. The observation that pre-culturing did not prevent occurrence of a lag phase at a high EDTA concentration (**Fig. 2.1** and **S4**) may provide a clue. Such a dilution event may cause stress, though the dilution factor is much smaller in the turbidostat (~5 %, compared to approximately 10 or 20-fold in flask experiments). Consistent with this interpretation, reducing the size of this dilution factor, by narrowing the turbidostat thresholds, led to an increase in growth rate (Supporting Information **Fig. S2.2**).

In a typical batch culture of *Synechocystis*, exponential growth – with a saturating supply of actinic light – is followed by a period of light-limited growth, often observable as a phase with 'linear' growth (139), and eventually the stationary phase commences when nutrients in the medium run out, provided sufficient light and carbon is available. It has been suggested (142) that phosphorus is limiting growth in BG-11, as it is supplied in amounts that are not compatible with the Redfield ratio (141) and phosphate is rapidly depleted from the medium. While these latter statements are true, they ignore the fact

that, based on the biomass composition reported by Kim *et al*. (2011), and this study, and the phosphorus content of BG-11, a maximum biomass density of only 0.37-0.48 gDW L^{-1} ($OD_{730} \approx$ 2.0-2.7) is theoretically possible, which can clearly be exceeded (see **Fig. 2.1** and **2.3**). Besides phosphorus, this also holds for other macronutrients supplied, i.e. nitrogen and sulfur, which allow for 1.98-2.28 gDW L^{-1} ($OD_{730} \approx$ 11.0-12.7) and 1.40-2.17 gDW L^{-1} ($OD_{730} \approx$ 7.7-12.1), respectively. All these OD values are exceeded with saturating illumination before the onset of stationary phase and the subsequent bleaching (i.e. values up to $OD_{730} \approx$ 16 can be reached). Clearly, the biomass composition of cells that were grown in nutrient-rich conditions does not accurately predict the limiting nutrient that forces cells to enter stationary phase. A possible explanation for the mismatch of measured yield and expected yield based on the biomass composition for phosphorus and nitrogen is that these components are stored inside the cell (e.g. as polyphosphate and cyanophycin, respectively) and thereby inflate the required amounts when predicted by the biomass composition of nutrient-rich cells. Under these conditions, i.e. in the log phase of a batch experiment in flasks, this is expected, but in an energy-limited continuous culture at high growth rate, it is not.

Here, we show that entry of a batch culture into the stationary phase in BG-11-PC medium, provided light and CO_2 are saturating, occurs due to sulfur limitation and causes rapid bleaching of the cells and cell death. Interestingly, this bleaching cannot be reverted by addition of sulfate after growth has halted and ROS levels peak (**Fig. 2.5**). This dramatic effect of sulfur limitation contrasts the effect of limitation in e.g. nitrogen, phosphorus and iron, suggesting that *Synechocystis* infrequently encounters sulfur limitation in its natural environment and that this cyanobacterium has no regulatory network to cope with this specific limitation. This makes sulfate a poor choice as the limiting nutrient in the growth medium, as it is not readily apparent from the appearance of the culture when this limitation starts, nor how it affects metabolism. Macronutrients that, upon depletion, cause a clear and reversible entry into stationary phase are more suited as a growth-limiting nutrient. Nitrogen starvation causes selective gradual degradation of the phycobilisomes, leading to a yellow-green appearance of the culture (158). Given the high nitrogen content of the medium, this element is the most economical choice to reduce to limiting levels if high cell densities are not required. Alternatively, sulfur can be increased to lift the sulfur limitation of high density cultures, which will then be limited by nitrogen instead (Supporting Information **Table S2.2**). In continuous culture, however, the biomass composition predicts that phosphorus will be limiting. Growth rate appears to be correlated with the size of the intracellular pools, in accordance with the Droop model (159). In a recent paper (160), it was proposed that *Synechocystis* enters stationary phase due to cell-cell interactions rather than self-shading or other nutrient limitation. However, the final density those authors observed when cells entered stationary phase was 0.12 gDW L^{-1} on average, which is far below what we observe (2.88 gDW L^{-1}), indicating that growth is halted for other, unknown, reasons in their experiments than it is here.

It is of great importance that culturing conditions are precisely defined in order to interpret the results of any given experiment, even beyond the necessity of being able to reproduce the result(s). Here, we show that the interpretation of measurements that is often taken for granted, such as of the optical density of a culture, is influenced by factors that can – and in most cases, will – change during an experiment, unless the experiment is designed with these factors in mind. From this, it follows that, ideally, studies should be done using fixed growth rates (i.e. in a chemostat or turbidostat) in order to avoid the great differences that can arise plainly from having a different growth rate. Other methods may be employed to obtain controlled growth rates in batch cultures, such as the recently described 'photonfluxostat' approach (150). At the very least an effort has to be made to account for differences that may arise from the resulting growth conditions, rather than from the variable of interest.

The reduction of chlorophyll content in faster growing cells, i.e. at higher incident light intensity, indicates that 'high' or 'low' incident light is relative to the cell density, and unless so high as to become inhibiting, growth rate essentially reflects light conditions in the absence of other limitations. This is illustrated by the growth curve shown in **Fig. 2.3** in which initially rapid growth is observed in what is commonly referred to as 'moderate' or even 'low' light intensities (~30 µmol photons m^{-2} s^{-1}) in culturing facilities with a light path-length of a few centimeters or more. Indeed, because of the low cell density at this point, such intensities are actually perceived by the cells as 'high light' and allow exponential growth of the cells at a high rate.

Growth rates of up to 0.15 h^{-1} have been reported for *Synechocystis* before, though it was not clear whether these could be sustained (150, 155). Here, we show that the maximum growth rate of *Synechocystis* in orange-red light is at least as high as 0.16 h^{-1} (4.3 h doubling time, see **Fig. 2.6**), which is almost twice the textbook value (8 h doubling time, ~0.09 h^{-1}). As shown by Du et al. 2016, an increase in dilution rate requires a proportional increase in light flux to maintain the same biomass density. In the presented chemostat data, the light intensity was kept the same which should result in lower biomass density with increasing dilution rate. However, the biomass density did not scale proportionally, i.e. the yield on light had dropped. This indicates that μ_{max} is likely to be close to 0.16 h^{-1}.

2.5   Acknowledgements

2.6   Supporting information

The Supporting Information **Dataset 1** is available upon request at pascal.vana@gmail.com.

Table S2.1. Composition of BG-11-PC and standard BG-11 in g L^{-1}. Compounds marked with an asterisk differ between the two media.

Compound	BG-11-PC	Standard BG-11
$NaNO_3$	1.5	1.5
K_2HPO_4	0.04	0.04
$MgSO_4 \cdot 7H_2O$	0.075	0.075
$CaCl_2 \cdot 2H_2O$	0.036	0.036
Na_2CO_3*	0	0.02
$FeCl_3 \cdot 6H_2O$*	0.004	0
Ammonium ferric citrate*	0	0.006
Citric acid*	0	0.006
EDTA $Na_2 \cdot 2H_2O$*	0.0186	0.001
Micronutrients	mg L^{-1}	
H_3BO_3	2.86	2.86
$MnCl_2 \cdot 4H_2O$	1.81	1.81
$ZnSO_4 \cdot 7H_2O$	0.222	0.222
$Na_2MoO_4 \cdot 2H_2O$	0.391	0.391
$CuSO_4 \cdot 5H_2O$	0.079	0.079
$Co(NO_3)_2 \cdot 6H_2O$	0.049	0.049

Table S2.2. Maximum OD_{730} reached in BG-11-PC with a single nutrient at half strength (left), all nutrients at half strength but supplemented with 0.01 ppm of a heavy metal (M, middle) or complete media (right).

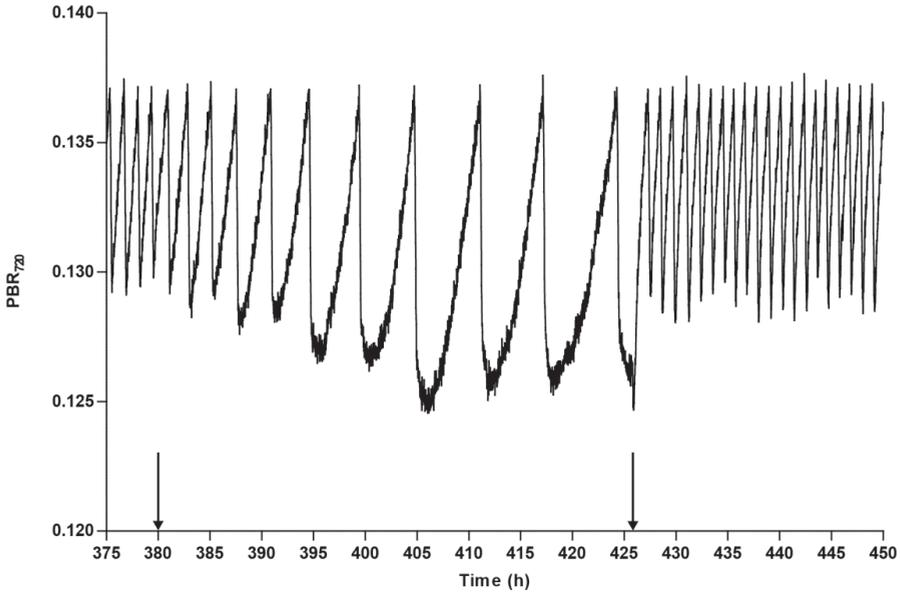| Named nutrient at half strength				BG-11-PC 0.5x + 0.01 ppm M		Complete media	
$ZnSO_4$	13.1	$MgSO_4$	8.4	$K(SbO)C_4H_4O_6$	5.4	BG-11 Sigma	15.5
$MnCl_2$	11.9	$CuSO_4$	13.8	$CrCl_3$	6.0	BG-11-PC	12.5
$FeCl_3$	12.2	$CaCl_2$	12.0	Na_2WO_4	5.7	BG-11-PC 0.5x	5.6
Na_2MoO_4	14.2	K_2HPO_4	13.4	NH_4VO_3	5.8		
H_3BO_3	11.9	$Co(NO_3)_2$	13.7	$NiSO_4$	6.7		
$NaNO_3$	18.7						

Fig. S2.1. Specific phenotype of *Synechocystis* during cultivation under shear stress originating from sparging in a turbidostat. At the first arrow, at 380 h, sparging was increased from 300 to 400 mL/min. At the second arrow, it was reduced to 50 mL/min. The lower and upper PBR_{720} thresholds were 0.130 and 0.137, respectively.
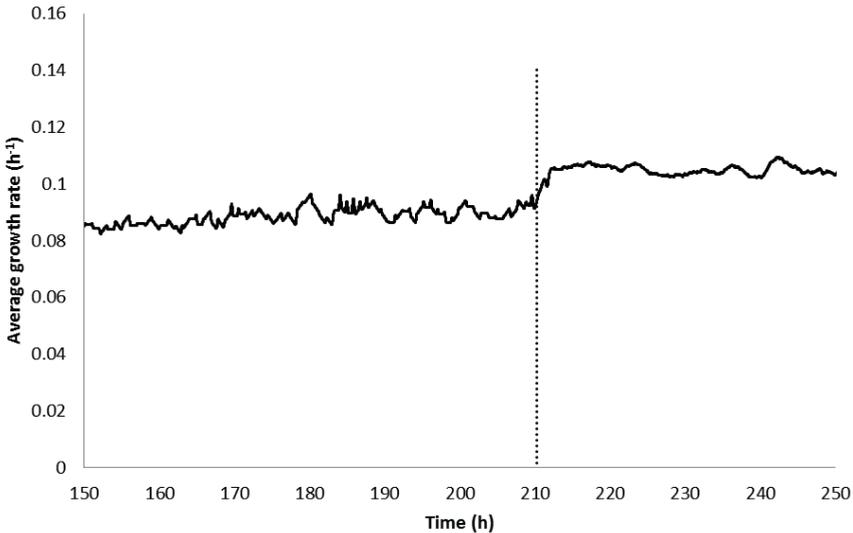

Fig. S2.2. *Synechocystis* growing in a turbidostat with varying threshold ranges around $OD_{730} \approx 0.4$, in BG-11-PC with increased K_2HPO_4 (10x) at 30 °C and a saturating light intensity of 400 μmol photons $m^{-2} s^{-1}$. The growth rate as determined by the effective dilution rate, based on the pump rate of fresh growth medium in a sliding window of 2 h, is plotted against time. The turbidostat control was switched from a relatively large range (±3.8 % of PBR_{720}) to a small range (±0.4 %) around the same set point at 210 h (dashed line). The average growth rate (±SD) before and after this switch was 0.089 ±0.008 h^{-1} and 0.105 ±0.002 h^{-1}, respectively.
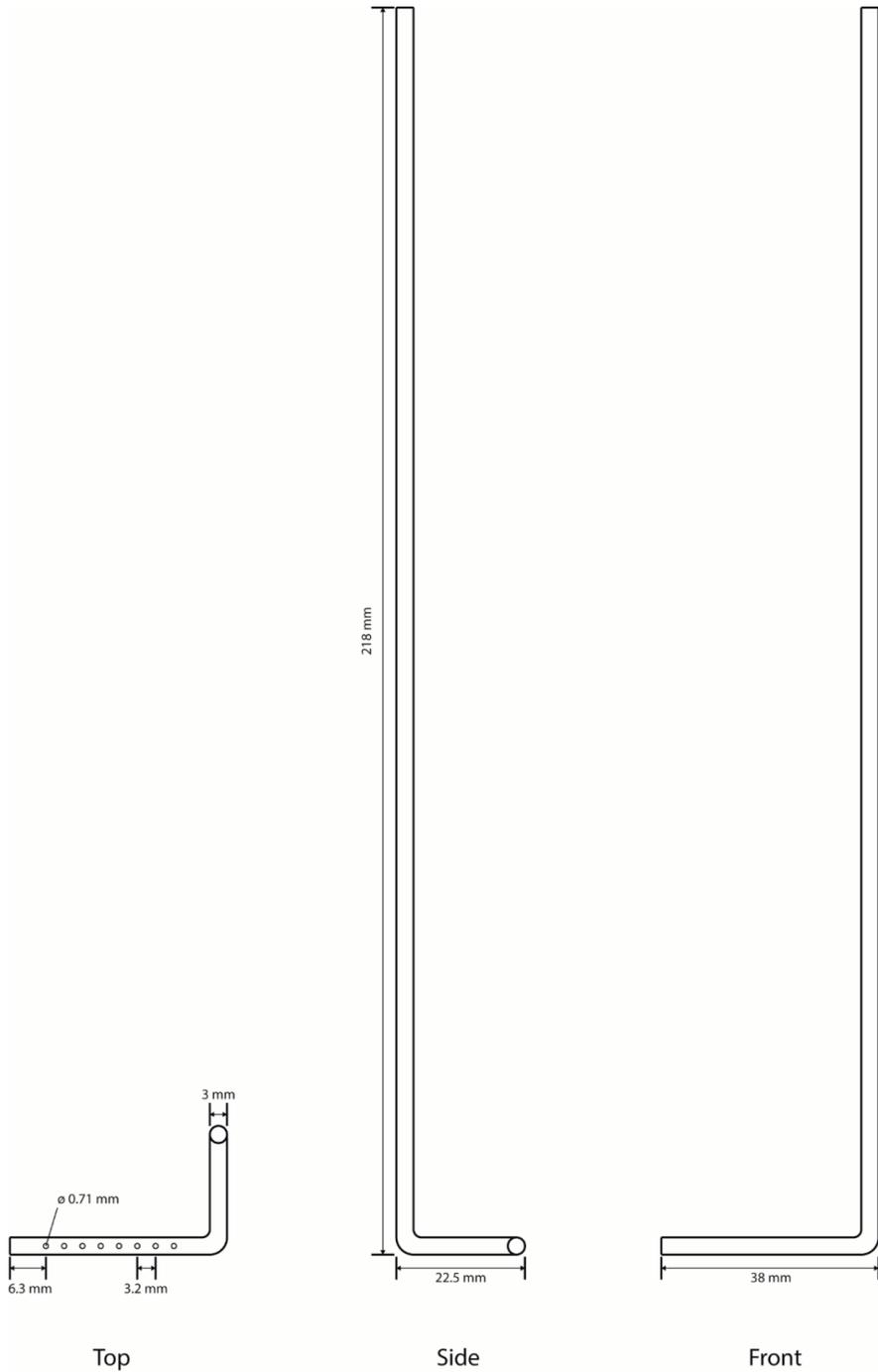
Fig. S2.3. Design of the new sparger. The bottom-end is almost closed, to facilitate sparging, yet allowing the sparger to be easily cleaned. It should be noted that fully closing the end reduces equal bubble distribution.